

Synthesis of Rhodamine TEMPO Conjugates via Isonitrile-Based Multicomponent-Reactions for Mitochondria-Targeted ROS-Detection in Cancer Cells

Haider N. Sultani,* Ibrahim M. Morgan, Hidayat Hussain, Haleh H. Haeri, Dariush Hinderberger, Goran N. Kaluđerović, and Bernhard Westermann*

A novel series of profluorescent rhodamine nitroxide conjugates are synthesized utilizing well-known isonitrile-based multicomponent reactions (IMCRs). The synthesized conjugates are rationally designed as mitochondria-targeting probes for the detection of reactive oxygen species in living cells. Herein, the synthesized probes demonstrate high selectivity to target the mitochondria of both of PC3- and NIH3T3-cells which represent cancer and normal cell lines. Attaching TEMPO nitroxide to rhodamine leads to fluorescence quenching, allowing for ROS detection and quantification. The prepared sensors provide a reliable method for distinguishing between different oxidative environments in living organisms through different levels of fluorescence to be measured. The use of the Ugi multicomponent reaction enables an efficient and versatile synthetic approach, offering significant advantages over previously reported methods for constructing ROS-detecting probes. The simplicity of the reaction setup and the ability to generate a diverse library of products by varying Ugi components make this protocol highly adaptable for further chemical modification and potential applications in biological systems.

questions and needs in the context of disease-related problems. Among the cellular processes which disclose a clear indication of nature, and the status thereof is the formation of reactive oxygen species (ROS). ROS include hydroxyl radicals and superoxide anions which represent oxygen radicals, although non-radical ROS also exist such as hydrogen peroxide and ozone. Approximately 1% of the oxygen taken up in our bodies by simple breathing is converted to ROS.^[1]

Excess generation of ROS causes cellular damage, which results in oxidative stress and ultimately cell death. As a result of excess ROS production, DNA damage may occur which may provoke gene mutations. In addition, many diseases are associated with excess ROS production such as neurodegenerative disease (Alzheimer's),^[2] hypertension,^[3] loss of cardioprotection,^[4] and hyperglycemia.^[5]

1. Introduction

Monitoring biological processes within cells is an ongoing process and modern analytical tools have been constantly developed to provide fast, reliable, and reproducible results to pressing

Indeed, ROS production by cancer cells is their major manifestation and due to its high metabolic activity compared to the normal cells presents the problem to be addressed.^[6] Therefore, an understanding of the reasons and conditions causing these distortions is a mandate to develop promising tools to

H. N. Sultani^[†], I. M. Morgan, H. Hussain, G. N. Kaluđerović, B. Westermann
 Department of Bioorganic Chemistry
 Leibniz-Institute of Plant Biochemistry
 Weinberg 3, 06120 Halle, Germany
 E-mail: hsultani@ipb-halle.de; bwesterm@ipb-halle.de

H. H. Haeri, D. Hinderberger
 Institute of Chemistry
 Physical Chemistry – Complex Self-Organizing Systems
 Martin Luther University Halle-Wittenberg
 von-Dankelmann-Platz 4, 06120 Halle, Germany
 G. N. Kaluđerović
 University of Applied Sciences Merseburg
 Eberhard-Leibnitz-Straße 2, 06217 Merseburg, Germany
 B. Westermann
 Institute of Chemistry
 Organic Chemistry
 Martin Luther University Halle-Wittenberg
 Kurt-Mothes-Strasse 2, 06120 Halle, Germany

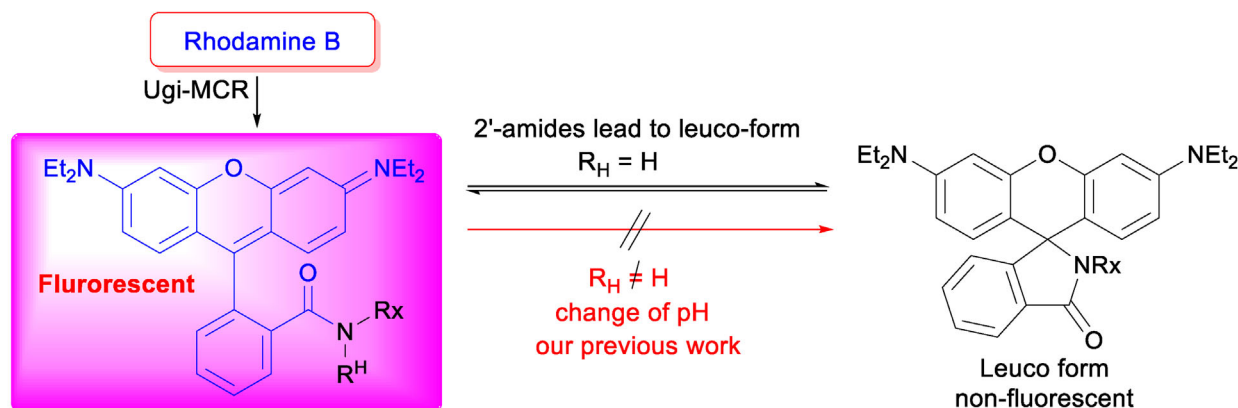
 The ORCID identification number(s) for the author(s) of this article can be found under <https://doi.org/10.1002/adsr.202400180>

^[†]Present address: College of Pharmacy, Al-Naji University, Baghdad, Iraq

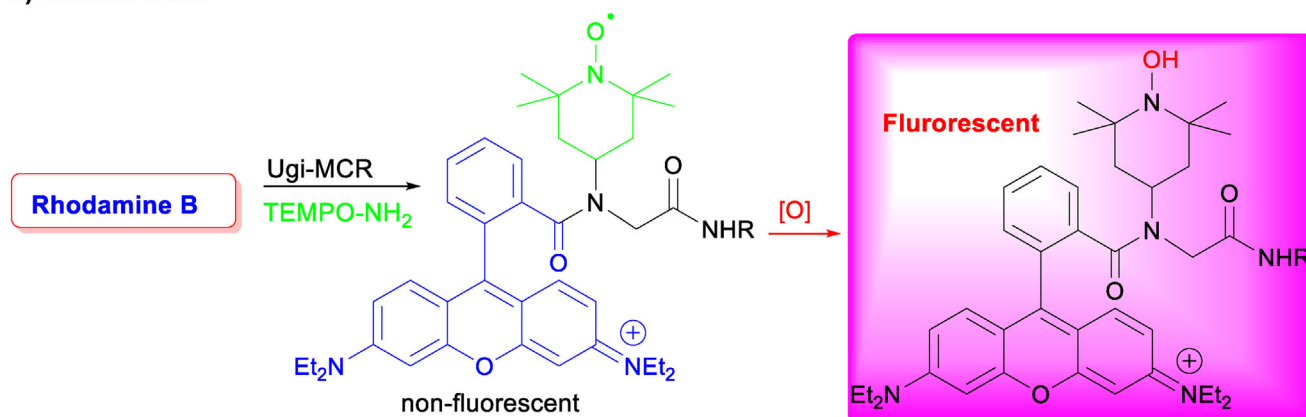
© 2025 The Author(s). Advanced Sensor Research published by Wiley-VCH GmbH. This is an open access article under the terms of the [Creative Commons Attribution](#) License, which permits use, distribution and reproduction in any medium, provided the original work is properly cited.

DOI: 10.1002/adsr.202400180

a) Previous work



b) Current work



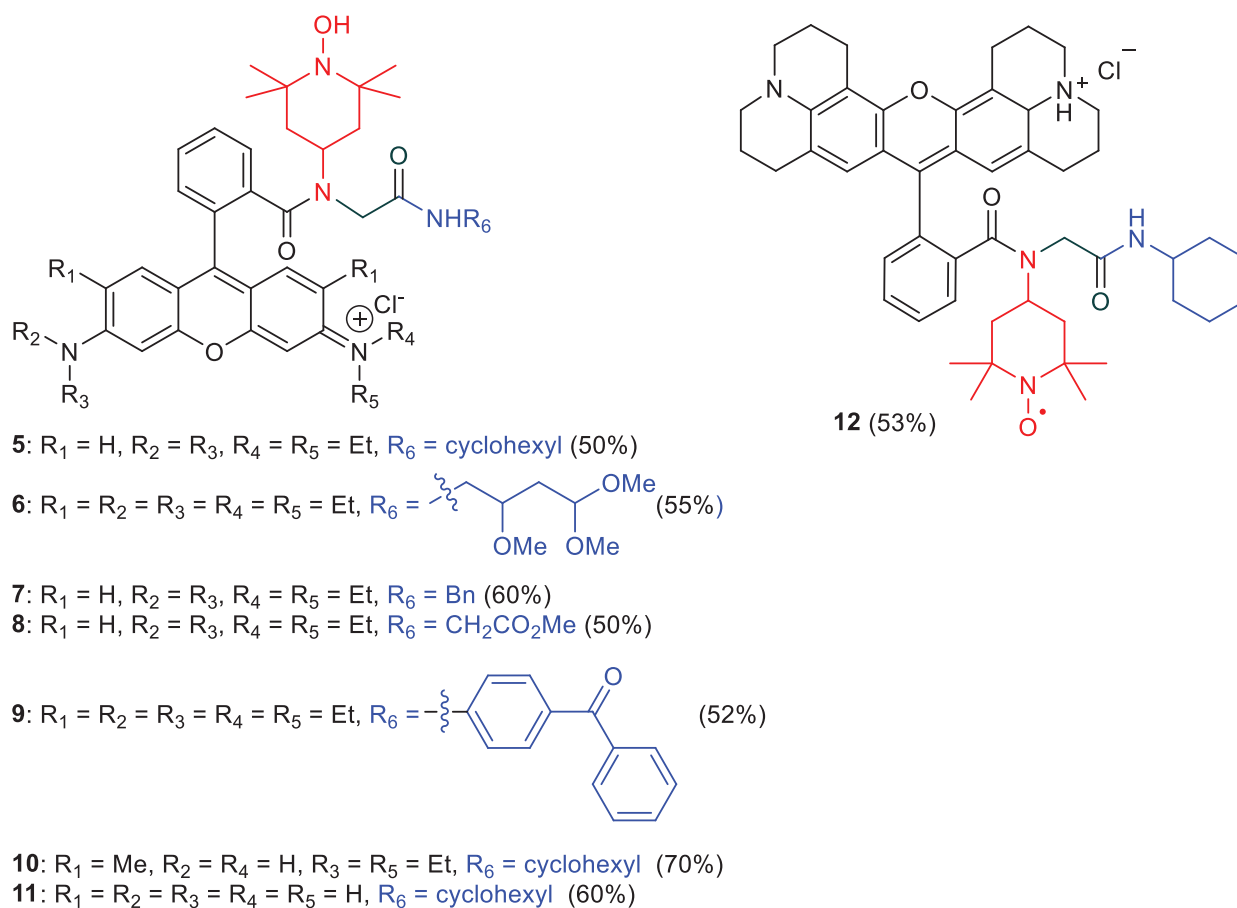
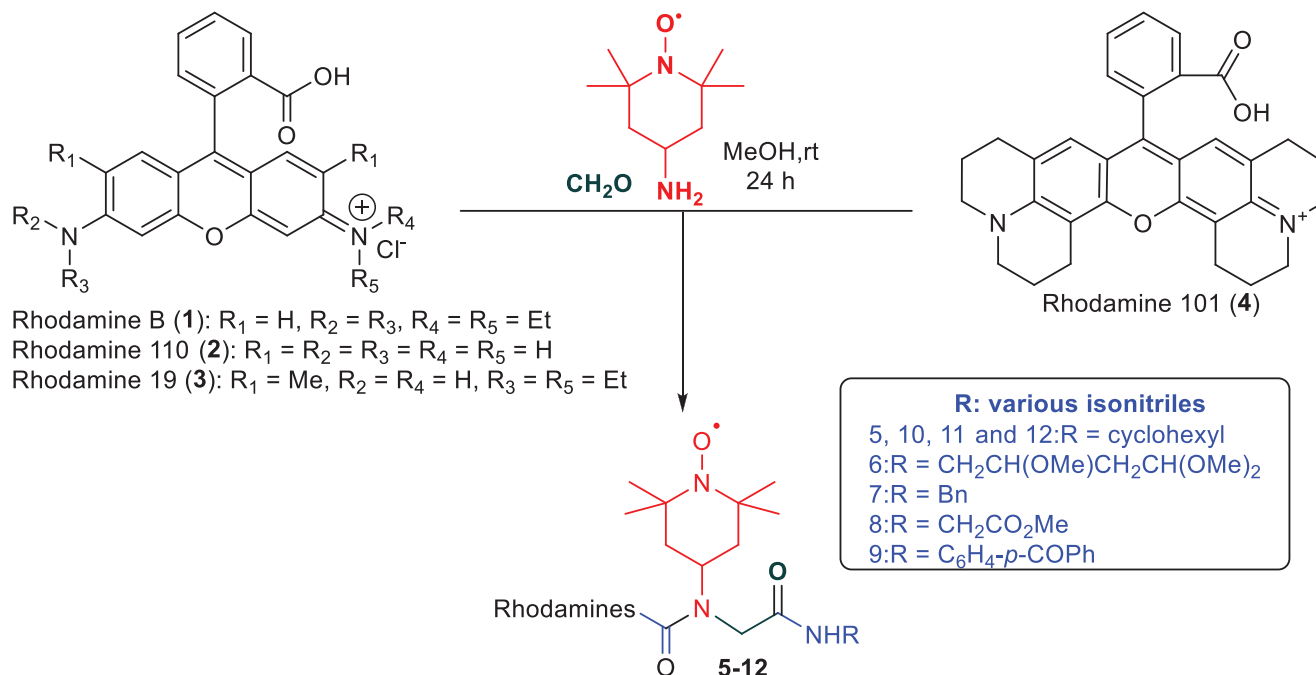
Scheme 1. Comparison of previous and current work.

counteract this situation. The localization of these processes to subcellular organelles is also indispensable. As the electron transport chain is located in the mitochondrial membrane, it is most likely that this organelle is a major source of ROS. Indeed 90% of ROS production takes place in the mitochondria, which are formed during oxidative phosphorylation, amino acid, and fatty acid metabolism, and hormone biosynthesis.^[7] Due to their high degree of inherent redox processes which starts with the flow of electrons from the electron transport chain to oxidize molecular oxygen to the radical oxygen species, mitochondria are a well-studied cell compartment.

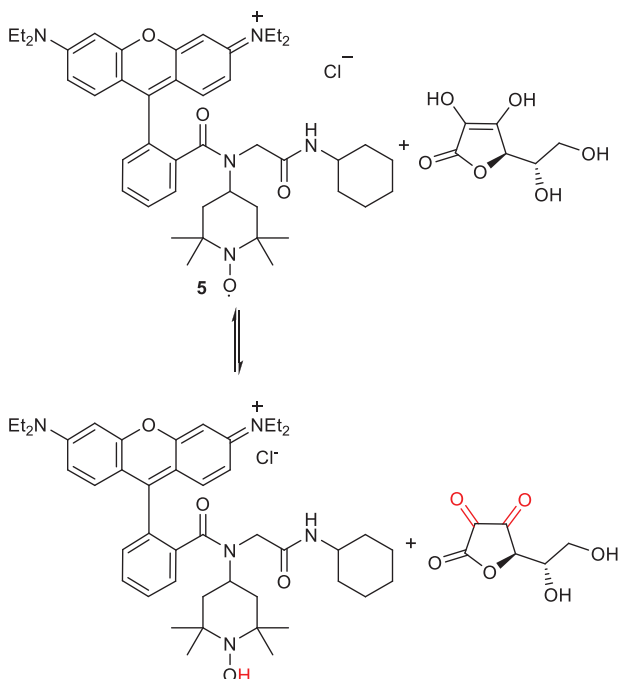
Numerous fluorophores for mitochondria targeting have been reported, such as fluorescein which is routinely used for protein labeling but suffers limited cellular permeability in studies involving living cells. In contrast, different rhodamine dyes; rhodamine 123, rhodamine B, basic violet 11, rhodamine 6G, and rhodamine 101, are excepted for their propensity to penetrate cells more readily than fluorescein, because of the negative plasma membrane potential within the cell cytoplasm. Moreover, the delocalized cationic π -system of rhodamines facilitates their accumulation in the mitochondria.^[8] In our studies to target mitochondria, the rhodamine fluorophore was selected, because it has been proven that such lipophilic cationic dyes are localized into that particular organelle, therefore acting as the fluorophore

as well as a targeting group.^[9] Moreover, rhodamines gained high attraction due to their desirable photophysical properties, such as; high quantum yield (ϕ) and high molar absorptivity (ϵ). In addition, due to their excellent photostability, rhodamines are widely used in biological studies^[10] and are also known to possess high chemical stability. Their stability toward pH, metal ions, anions, and thiols lent credence to their most important feature being their stability toward reactive oxygen species.^[11–13] In close proximity to the dye, we envisioned installing a 2,2,6,6-Tetramethylpiperidinyloxy nitroxide radical (TEMPO)-moiety for maximum quenching efficiency since the quenching of the fluorophore is highly dependent on the distance between the nitroxide radical relative to the fluorescent tag.^[14] One of the applications of nitroxides is their conjugation to fluorophores and to utilize these conjugates as pre-fluorescent dual-functional (spin and fluorescence) sensor molecules.^[15–17] Nitroxides are known to act as profluorescent probes through their ability to quench the excited state of fluorescent tags.^[18–21]

In the current study we describe the preparation of rhodamine TEMPO conjugates as mitochondria targeting probes. Many reports showed that rhodamine dyes, tend to accumulate and localize in the mitochondria.^[22,23] However, the major drawback of rhodamine chemistry is that its analogs are pH-sensitive, and rhodamine secondary amides lead to the leuco-form



Scheme 2. Preparation of spin-labeled probes 5–12.



Scheme 3. Ascorbic acid reduction of probe 5.

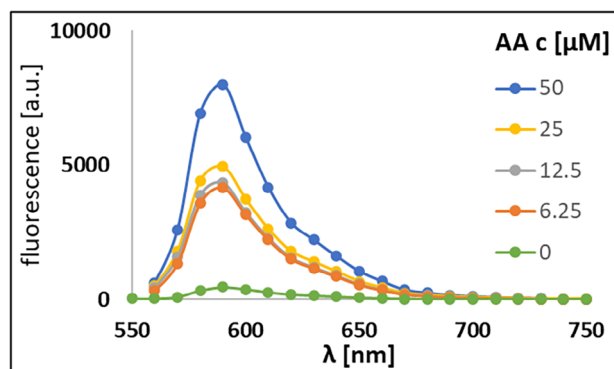


Figure 1. Fluorescence response of spin-labeled probe 5 (50 μM) to ascorbic acid (AA).

(non-fluorescent) via intramolecular cyclization (Scheme 1). In earlier studies, we demonstrated that utilization of rhodamine in Ugi-reactions leads to peptoids that cannot be transformed into the leuco form upon a change of pH (Scheme 1).^[24] The Ugi-reaction offers the possibility to use TEMPO-NH₂. The adduct derived is thus non-fluorescent due to the quenching by the radical. However, upon oxidation, this probe will turn into a fluorescent analyte able to monitor the ROS upon change of intensity of the Ugi-adduct. In addition, the incorporation of the TEMPO-radical also offers the possibility to use this sensor as a double readout probe, the second readout obtained from Electron Paramagnetic Resonance (EPR) spectroscopy. EPR spectroscopy is a well-established, powerful technique with a wide range of applications. It is a highly precise, non-destructive method that needs very small amounts of the sample (10–100 μL ranges). All these properties make EPR suitable for biological kinds of purposes. EPR is based on monitoring the interaction of unpaired

electrons with microwave irradiations in the presence of a magnetic field. Therefore, it could be utilized to find out not only the level of ROS, but RNS (Reactive Nitrogen Species) in cellular systems, as well. About the role of EPR in detecting and quantifying ROS in biological media, there are detailed reviews elsewhere.^[25–27]

The Ugi multicomponent reaction (U-MCR) is a well-established one-pot synthetic protocol to achieve diversity in only one synthetic operation. The scope is rather broad, and a variety of functional groups can be used in the carboxylic acid, amine, and isonitrile components without the need for protection strategies and activation, with water as the sole byproduct. Its applicability toward the synthesis of bioactive compounds has been demonstrated in several examples.^[28–31] In earlier studies, we also demonstrated that the conditions of the Ugi-reaction do not interfere with the TEMPO-radical, keeping the radical character intact throughout the synthesis.^[32,33] This study advances the development of mitochondria-targeting ROS probes by leveraging the unique properties of rhodamine fluorophores and nitroxide radicals through an efficient and modular synthetic approach. Employing the Ugi multicomponent reaction in this study ensures enhanced chemical stability, dual detection capabilities via fluorescence and EPR spectroscopy, and adaptability for structural diversification through the Ugi reaction. These attributes make it a promising tool for bioimaging, oxidative stress monitoring, and redox biology studies, with potential applications in understanding and diagnosing oxidative stress-related diseases.

2. Results and Discussion

2.1. Synthesis and Characterization

For this study, we envisioned using the TEMPO radical as the amine component. To ensure a close distance and maximum quenching of the radical to the fluorophore, rhodamine B was selected as an acid component in the U-MCR, and formaldehyde was used as the carbonyl compound to avoid any formation of stereoisomers. For diversification 1) rhodamine B, 2) rhodamine 110, 3) rhodamine 19 were used (Scheme 2). Various isonitriles comprising cyclohexyl, benzyl, and benzophenone groups were used to generate a library of rhodamine TEMPO conjugates. The U-MCR was also carried out with convertible isonitriles having an ester group and an IPB isonitrile which allows for post-U-MCR modification.^[34,35] All U-MCRs were carried out in methanol as solvent at room temperature under ambient conditions. The yields of spin-labeled probes 5–12 (Scheme 2) ranged from $\approx 50\%$ to 70%. These good yields clearly prove the versatility of the U-MCR approach to achieve a broad range of rhodamine radical sensors in just one transformation. The nature of the carboxylic acid part had no big impact on the product formation.

2.2. UV, EPR, and NMR Spectroscopic Properties of the Spin-Labeled Probe 5

We selected spin-labeled probe 5 to test whether it can be reduced to the corresponding hydroxylamine thereby facilitating the rhodamine dye to gain back its fluorescence. For this purpose, we

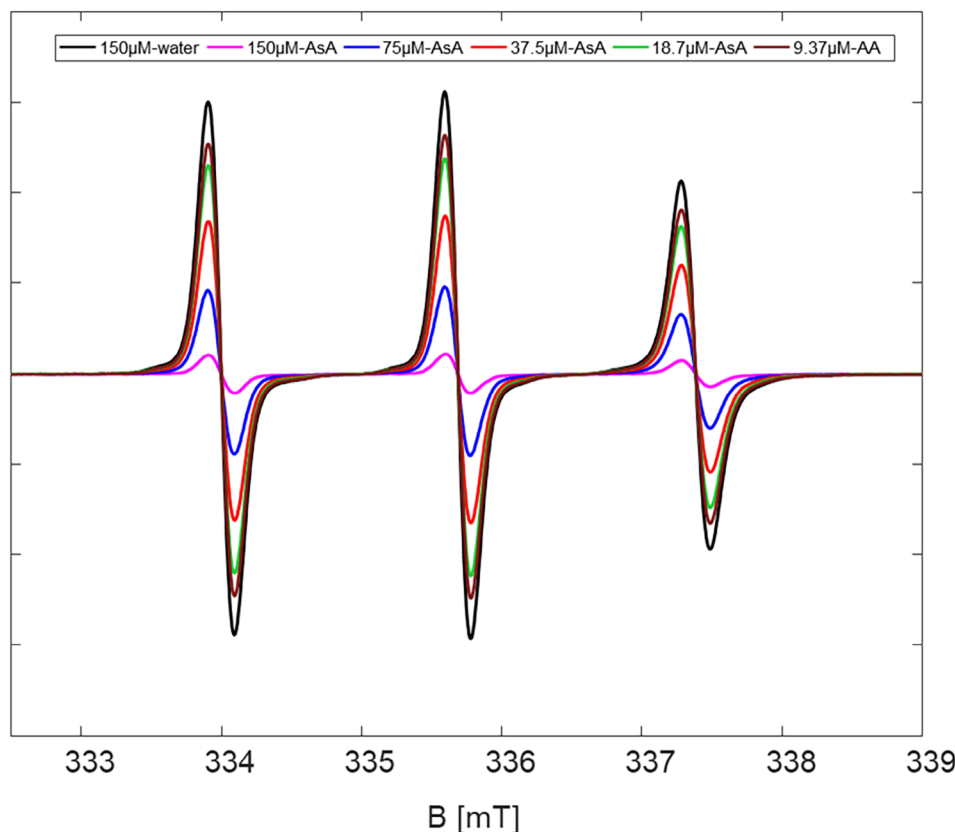


Figure 2. cw-EPR spectra of the stepwise reduction of spin-labeled probe 5 by ascorbic acid (AA). The black spectrum represents probe 5 in water (reference) before the addition of AA.

have selected ascorbic acid (AA) as the reducing agent in different concentrations (Scheme 3). The spectral characteristics of the synthesized spin-labeled probe 5 were tested in the absence and presence of AA. Both EPR and fluorescence spectroscopy were used to monitor the reaction at different concentrations of AA. The results show a dose-dependent response relationship between AA and the probe 5. Before AA was added almost no fluorescence was recorded for probe 5 (50 μM in methanol) as seen in Figure 1. As the molar ratio of AA slowly increased in stages from 6.25 up to 50 μM while keeping the concentration of probe 5 constant (50 μM), the fluorescent intensity increased as shown in Figure 1. The EPR spectra were recorded in a stepwise addition of AA to probe 5, as well (Figure 2). After the addition of AA to compound 5 (150 μM) in a stepwise manner (AA: 75, 37.5, 18.75 and finally 9.37 μM), the intensity of the typical three lines of the nitroxide radical of probe 5 decreased until an almost full quenching of the EPR signal occurs (Figure 2). The simulated EPR spectrum of probe 5 in water showed an isotropic hyperfine coupling (Aiso) of 47.66 MHz and resulted in an isotropic g-value of 2.0057 (Figure S4, Supporting Information). Both of these properties are in agreement with the typical nitroxide isotropic values in a polar environment.^[36–38] The Easyspin software package is used for the simulations.^[39]

In order to record the NMR spectra of probe 5, the nitroxide moiety must be reduced to its corresponding hydroxylamine. The reduction of the spin-labeled probe 5 was performed in situ utilizing the reducing agent AA (Scheme 3). The reaction

was monitored via NMR for 66 min (Figure S1, Supporting Information).

2.3. Biological Safety of the Synthesized Spin-Labeled Probes (5–8)

Before investigating the ability of the spin-labeled probe 5 to detect the ROS in cancer cell lines, the safety of the synthesized probes 5–8 was first confirmed. Both, embryonic mouse fibroblast NIH3T3 cells which represent mouse normal fibroblasts as well and human prostate PC3 cancer cells which represent human prostate cancer were used as models (MTT/3-(4,5-dimethylthiazol-2-yl)-2,5-diphenyl tetrazolium bromide and CV/crystal violet assays) to determine the viability of the cells. The tested spin-labeled probes 5–8 did not significantly affect the normal cell growth at 0.1 and 1 μM as well as the mitochondrial function compared to untreated cells. Thus, the compounds in their used concentrations were found to be non-toxic against the selected tumor and normal cells (Figure 3). The spin-labeled probes 5–8, showed a high degree of safety and were tolerated by both the PC3 prostate tumor and the normal fibroblast NIH3T3. The results encouraged us to continue with the follow-up studies as described before. We envisioned to use spin spin-labeled probe 5 as our model probe although spin-labeled probes 6 and 7 performed very well although the theory of our study required one representative probe.

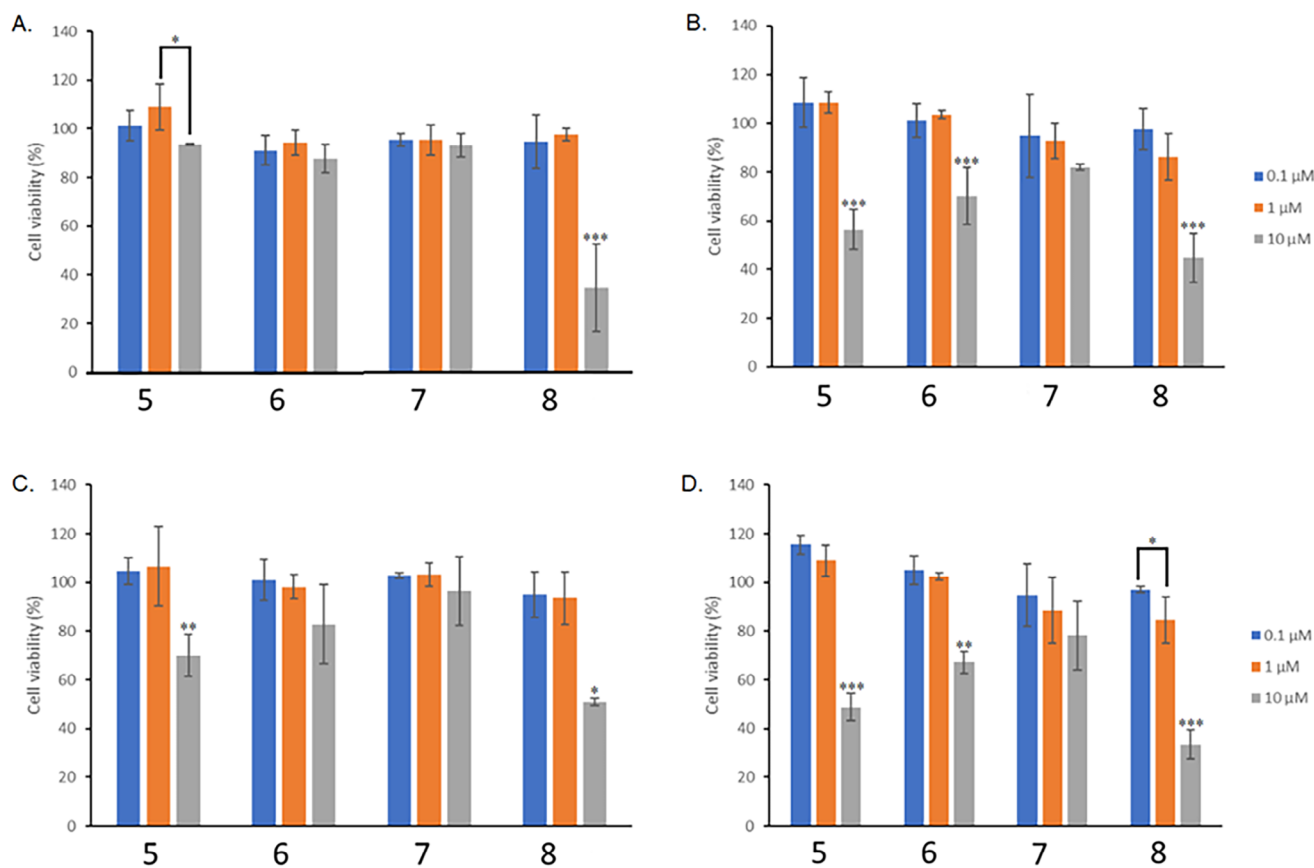


Figure 3. Cell viability was determined after 48 h of treatment with probes of A) NIH3T3 and B) PC3 cells evaluated with MTT assay, C) NIH3T3 and D) PC3 cells evaluated with CV assay. One-way ANOVA, * $p < 0.05$, ** $p < 0.01$, *** $p < 0.001$.

2.4. ROS Detection of the Spin-Labeled Probe 5 via Flow Cytometry Analysis

To evaluate the ROS-detection potential of TEMPO-containing probes, cells were treated with spin-labeled probe 5, and flow cytometry analysis was performed (Figure 4). Briefly, PC3 and NIH3T3 were stained with dihydro rhodamine (DHR) dye, then co-treated with the spin-labeled probe 5 to investigate and compare the ROS production in the normal as well as in the tumor cells. DHR dye is an uncharged and non-fluorescent ROS indicator and upon interaction with ROS, the dye is oxidized to cationic rhodamine, which localizes in the mitochondria and exhibits green fluorescence (Scheme 4).

Two different detection channels with different excitation/emission wavelengths were used to record the fluorescence of both DHR and the spin-labeled probe 5. A FITC detection channel was used for DHR with excitation/emission wavelengths of 488nm/520nm and supported by a Texas red detection channel with excitation/emission wavelengths 561nm/610nm^[40] used for the spin-labeled probe 5. As a positive control, cells co-treated with rhodamine and DHR were used. In theory, when cells are treated with rhodamine alone, high fluorescence is expected to be seen for both, PC3 and NIH3T3 cell lines. From DHR detection it can be seen that the ROS production is more prominent in the tumor PC3 than in normal NIH3T3 cells (Figure 4), as expected.

Namely, the difference in the fluorescence shift corresponds to the level of ROS species production. When the cells were double stained with rhodamine and DHR, no correlation between ROS-levels in normal and tumor cells was found as anticipated. In contrast, the cells co-treated with DHR and spin-labeled probe 5 exhibited a high correlation between ROS-level and fluorescence shift. The fluorescence intensity is concentration-dependent due to the fact that the nitroxide radical is being reduced to its corresponding hydroxylamine upon interaction with ROS thereby losing its ability to quench the fluorescence of rhodamine (Figure 4).

2.5. Mitochondria Targeting of the Spin-Labeled Probe 5

Localization of the novel spin-labeled probe 5 in the cells was determined using fluorescence microscopy (Figure 5). The tumor PC3 as well as normal NIH3T3 cells were treated with MitoTracker Green and subsequently with rhodamine, as control, and the spin-labeled probe 5, respectively. The images obtained by fluorescent microscopy showed that rhodamine localizes in the mitochondria (Figures 5A and 6A).^[22,23] As shown in flow cytometry experiments, independently from the ROS-level the intensity of rhodamine fluorescence is similar in NIH3T3 and PC3 cells. NIH3T3 cells stained with the spin-labeled probe 5 did not show fluorescence (Figure 6.B). On the other hand, PC3 cells

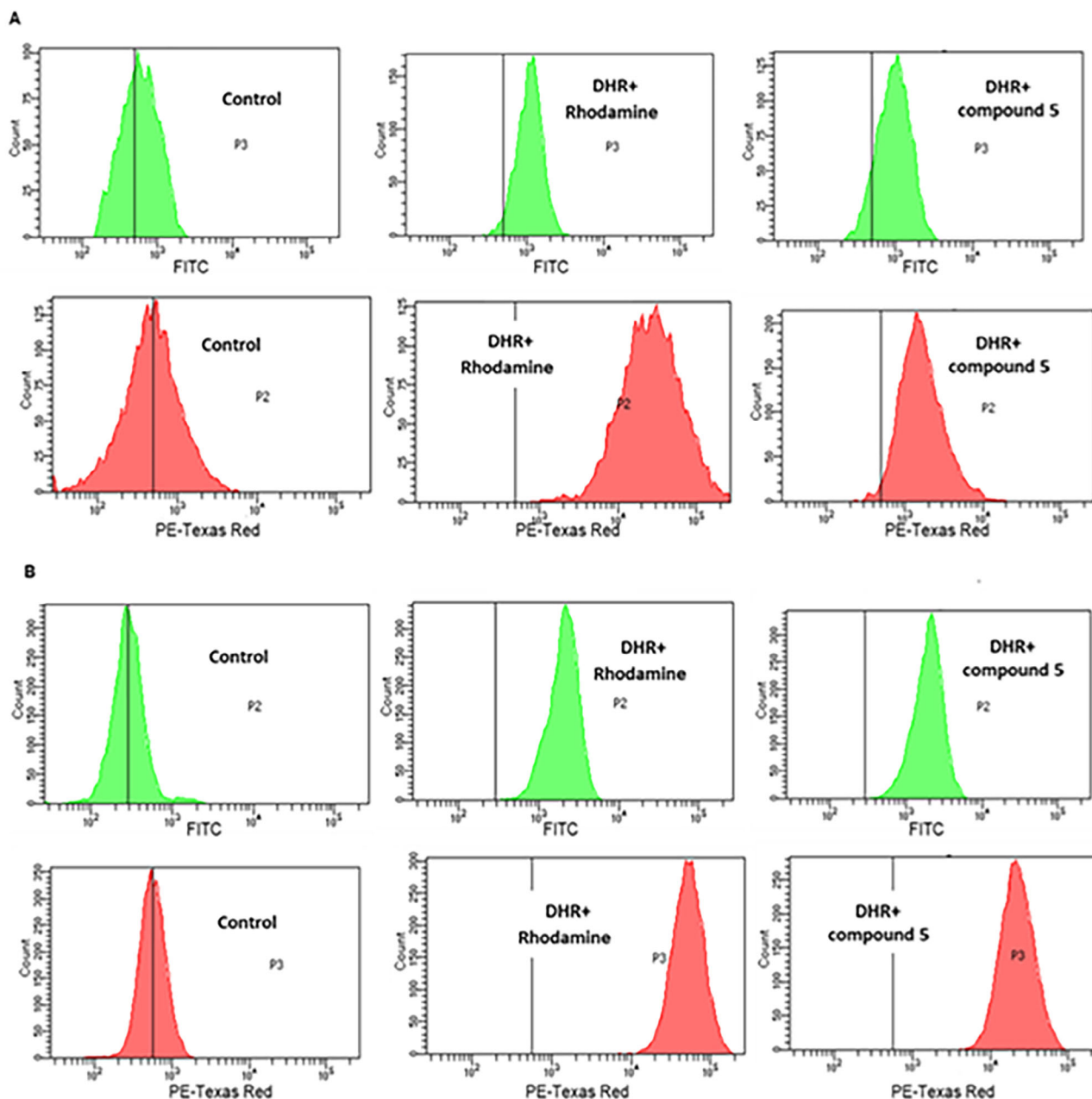
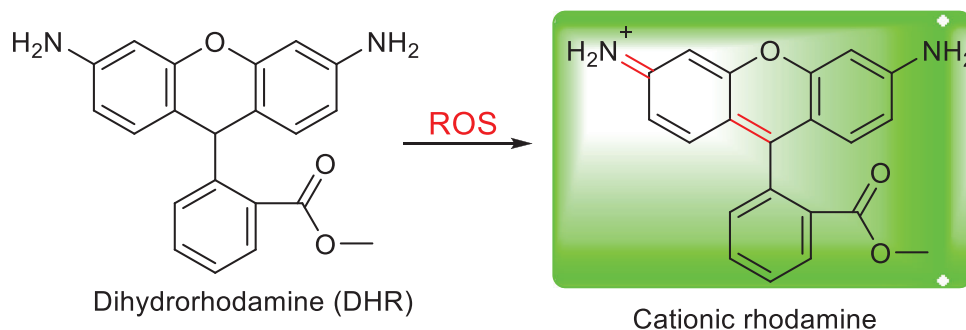


Figure 4. Flow cytometry analysis of A) NIH3T3 and B) PC3 cells double stained with DHR (10 min) and spin-labeled probe 5 (45 min).



Scheme 4. DHR for ROS detection.

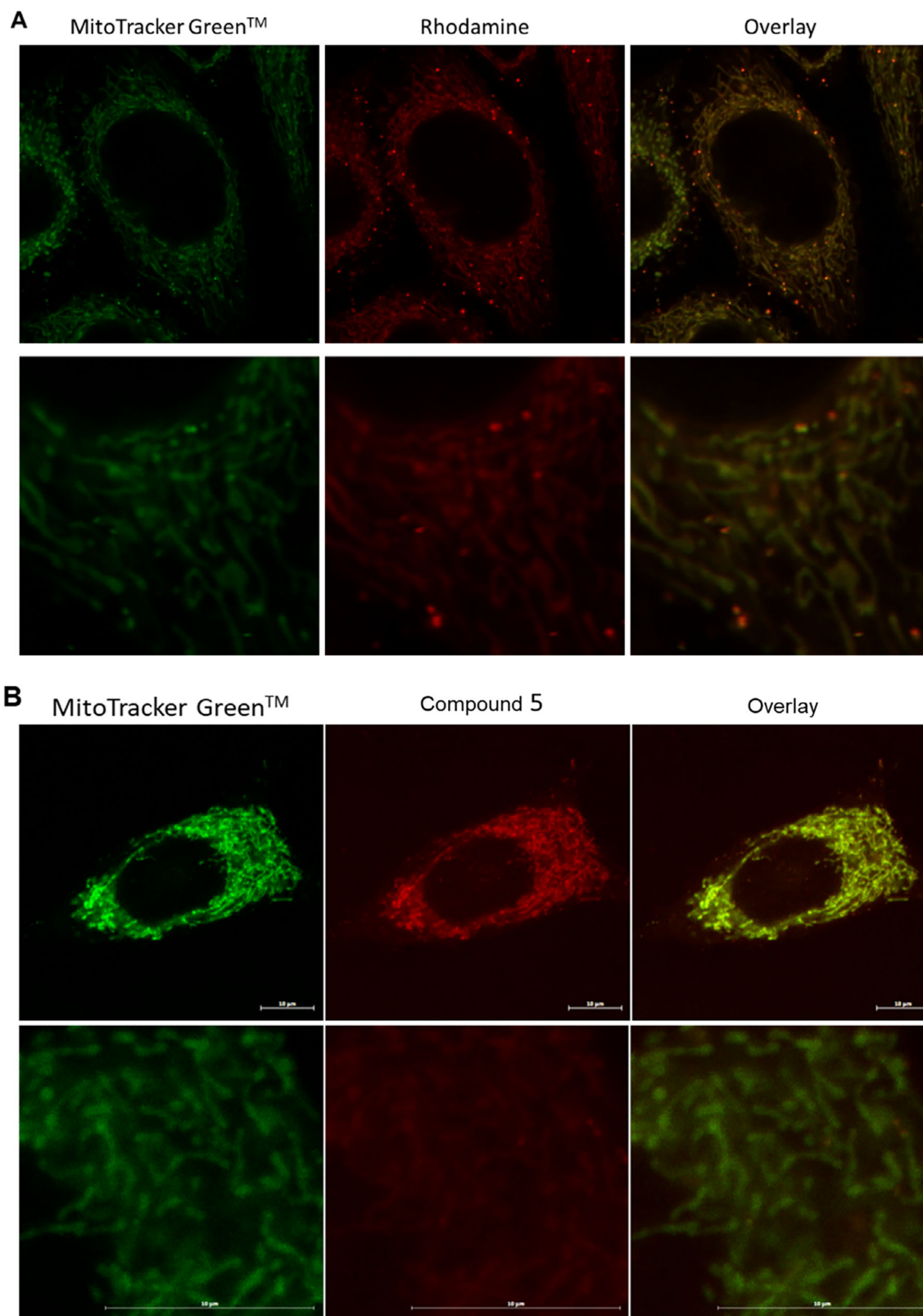


Figure 5. Fluorescence microphotographs: PC3 cells stained with MitoTracker Green (FITC channel) and rhodamine A; Texas Red channel) or spin-labeled probe 5 B; Texas Red channel).

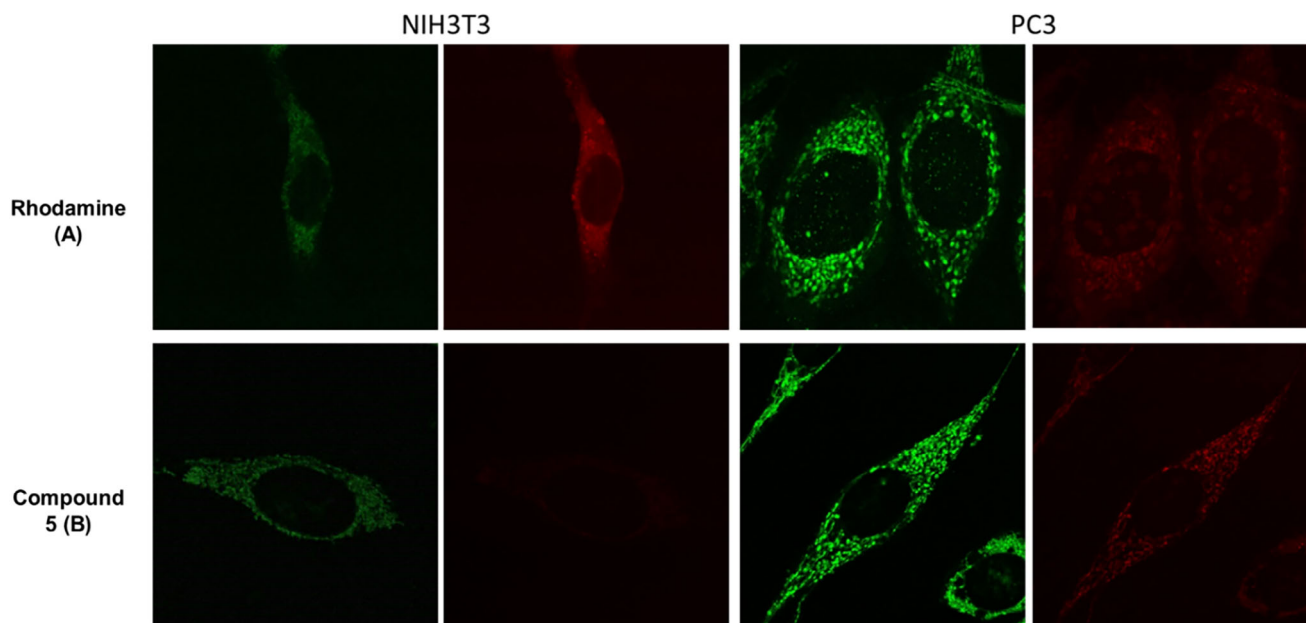


Figure 6. Fluorescence microphotographs: comparison of NIH3T3 and PC3 cells stained with MitoTracker Green (FITC channel) and rhodamine (Texas Red channel) or spin-labeled probe 5 (Texas Red channel).

treated with spin-labeled probe 5 exhibited high fluorescent intensity (Figure 5.B). This difference in the fluorescence intensity, in agreement with flow cytometry data, is due to the higher production of ROS by PC3 than NIH3T3 cells. The distribution panel of the spin-labeled probe 5 is the same as MitoTracker Green, a commercial stain that localizes exclusively the mitochondria.

2.6. Mitochondria Localization of Spin-Labeled Probe 5 via EPR Measurements

The ROS level of the three cellular moieties (whole cell, cytosolic extract, and mitochondria extract) in tumor PC3 cells was monitored at room temperature by EPR measurements. In addition to the aforementioned cellular compartments, the spectra of the control cells (NIH3T3) were recorded as well (Figure 7). The whole cells or compartments of interest (cytosol and mitochondria) were incubated with the probe 5 for 30 min at room temperature and then the samples were delivered to the EPR capillaries and were measured. Longer incubation times (up to 24 h) did not affect the final results. The synthesized probe 5 was found to be still active in whole cell and cytosolic extract samples while there was no signal in the mitochondria extract, neither for the control nor for the tumor cells. This is an indication that the ROS level in the mitochondria is higher than the other two compartments so the nitroxide is reduced to its hydroxylamine form. The diminished signal in mitochondria is well correlated to the corresponding increase of the fluorescence in the mitochondria as the nitroxide has lost its ability to quench the fluorescence of Rhodamine.

3. Conclusion

It is clearly evident that the Ugi-multicomponent reaction can be used as a simple and elegant synthetic protocol to develop new

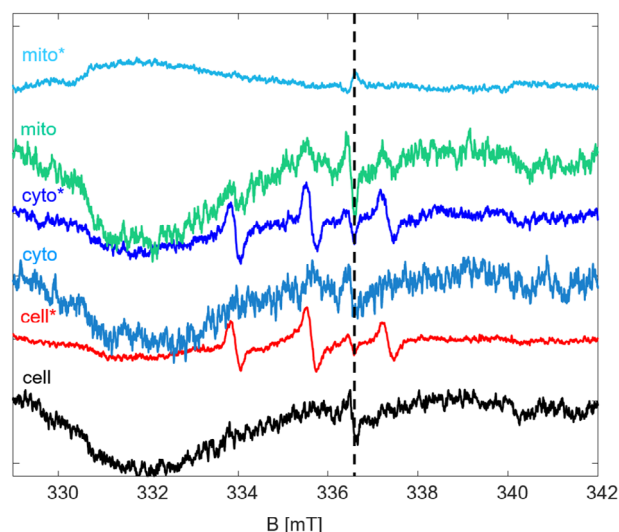


Figure 7. cw-EPR spectra of the NIH3T3 control and PC3 cancerous cells (assigned by star sign). The recorded spectra for whole cell, cytosolic extract, and mitochondria extract are given. The EPR characteristic parameters (A_{iso} and g_{iso}) are identical to those of probe 5. The signal at the field position denoted by the dashed line ($g_{iso} = 2.0012$) stems from defect centers in the used EPR capillaries.

rhodamine nitroxide probes for cellular ROS detection. The results were confirmed using different methods including flow cytometry, fluorescent imaging, and EPR spectroscopy. Probe 5 exhibited high selectivity toward the ROS and the high fluorescence shift can be seen in the PC3 cancer cell line with almost no fluorescence for the NIH3T3 cell line. The innovative TEMPO-probe can be successfully applied for the detection of ROS-levels using flow cytometry as well as localization of mitochondria in living

cells in vitro. The rhodamine-treated cells showed no difference in the intensity of the fluorescence between both cell lines while the spin-labeled probe 5 treated cells showed the presence of fluorescence in the case of PC3 cells since the TEMPO nitroxide is sensitive to ROS and presents to a larger degree in tumors than in normal cells. The findings from this study provide a strong foundation for the development of advanced bioimaging sensors for oxidative stress-related diseases. The dual fluorescence and EPR detection mechanism offers a more robust and versatile strategy for distinguishing oxidative environments in living cells, with potential applications in early cancer detection and therapeutic monitoring. Additionally, the adaptability of the Ugi multicomponent reaction enables further probe modifications, opening avenues for targeted imaging, antibody conjugation, and potential in vivo studies. These results underscore the promise of rhodamine nitroxide-based probes in biomedical research and diagnostic advancements.

Supporting Information

Supporting Information is available from the Wiley Online Library or from the author.

Acknowledgements

The authors thank Heike Schimm for technical support (EPR spectroscopy). This work was financially supported in part by the European Regional Development Fund (ERDF ZS/2016/06/79740).

Open access funding enabled and organized by Projekt DEAL.

Conflict of Interest

The authors declare no conflict of interest.

Data Availability Statement

The data that support the findings of this study are available in the supplementary material of this article.

Keywords

bioimaging, EPR, mitochondria-targeting sensors, multicomponent reactions (MCRs), rhodamine TEMPO conjugates, ROS detection

Received: November 23, 2024

Revised: March 14, 2025

Published online: April 17, 2025

- [1] S. Ban, H. Nakagawa, T. Suzuki, N. Miyata, *Bioorg. Med. Chem. Lett.* **2007**, *17*, 1451.
- [2] X. Chen, C. Guo, J. Kong, *Neural Regen. Res.* **2012**, *7*, 376.
- [3] A. E. Dikalova, I. A. Kirilyuk, S. I. Dikalov, *Redox Biol.* **2015**, *4*, 355.
- [4] N. Escobales, R. E. Nuñez, S. Jang, R. Parodi-Rullan, S. Ayala-Peña, J. R. Sacher, E. M. Skoda, P. Wipf, W. Frontera, S. Javadov, *J. Mol. Cell. Cardiol.* **2014**, *77*, 136.
- [5] C. M. Volpe, P. H. Villar-Delfino, P. M. Dos Anjos, J. A. Nogueira-Machado, *Cell Death Dis.* **2018**, *9*, 119.
- [6] S. Kumari, A. K. Badana, R. Malla, *Biomark. Insights* **2018**, *13*, 1177271918755391.
- [7] R. S. Balaban, S. Nemoto, T. Finkel, *Cell* **2005**, *120*, 483.
- [8] L. F. Mottram, S. Forbes, B. D. Ackley, B. R. Peterson, *Beilstein J. Org. Chem.* **2012**, *8*, 2156.
- [9] Q. A. Best, A. E. Johnson, B. Prasai, A. Rouillere, R. L. McCarley, *ACS Chem. Biol.* **2016**, *11*, 231.
- [10] M. Beija, C. A. Afonso, J. M. Martinho, *Chem. Soc. Rev.* **2009**, *38*, 2410.
- [11] S. Kenmoku, Y. Urano, H. Kojima, T. Nagano, *J. Am. Chem. Soc.* **2007**, *129*, 7313.
- [12] Y. Xiang, A. Tong, *Org. Lett.* **2006**, *8*, 1549.
- [13] B. Tang, L. Yin, X. Wang, Z. Chen, L. Tong, K. Xu, *Chem. Commun.* **2009**, 5293.
- [14] C. Aliaga, P. Fuentealba, M. C. Rezende, C. Cárdenas, *Chem. Phys. Lett.* **2014**, *593*, 89.
- [15] A. D. Verderosa, R. Dhoubi, K. E. Fairfull-Smith, M. Totsika, *Antibiotics* **2019**, *8*, 19.
- [16] K. Hideg, T. Kálai, C. P. Sár, *J. Heterocycl. Chem.* **2005**, *42*, 437.
- [17] M. Jia, Y. Tang, Y. F. Lam, S. A. Green, N. V. Blough, *Anal. Chem.* **2009**, *81*, 8033.
- [18] D. S. Weiss, *J. Photochem.* **1976**, *6*, 301.
- [19] S. Chattopadhyay, P. Das, G. L. Hug, *J. Am. Chem. Soc.* **1983**, *105*, 6205.
- [20] O. L. Gijzeman, *J. Chem. Soc., Faraday Trans. 2* **1974**, *70*, 1143.
- [21] M. M. Green, C. Andreola, B. Munoz, M. P. Reidy, K. Zero, *J. Am. Chem. Soc.* **1988**, *110*, 4063.
- [22] N. Morimoto, R. Takei, M. Wakamura, Y. Oishi, M. Nakayama, M. Suzuki, M. Yamamoto, F. M. Winnik, *Sci. Rep.* **2018**, *8*, 1128.
- [23] P. Reungpatthanaphong, S. Dechsupa, J. Meesungnoen, C. Loetchutinat, S. Mankhetkorn, *J. Biochem. Biophys. Methods* **2003**, *57*, 1.
- [24] S. Brauch, M. Henze, B. Osswald, K. Naumann, L. A. Wessjohann, S. S. van Berkel, B. Westermann, *Org. Biomol. Chem.* **2012**, *10*, 958.
- [25] R. Gulaboski, V. Mirčeski, R. Kappl, M. Hoth, M. Bozem, *J. Electrochem. Soc.* **2019**, *166*, G82.
- [26] Y. Zhang, M. Dai, Z. Yuan, *Anal. Methods* **2018**, *10*, 4625.
- [27] S. Suzen, H. Gurer-Orhan, L. Saso, *Molecules* **2017**, *22*, 181.
- [28] B. Westermann, S. Dörner, *Chem. Commun.* **2005**, *16*, 2116.
- [29] R. Echemendía, A. F. de La Torre, J. L. Monteiro, M. Pila, A. G. Corrêa, B. Westermann, D. G. Rivera, M. W. Paixão, *Angew. Chem., Int. Ed. Engl.* **2015**, *54*, 7621.
- [30] Y. Méndez, G. De Armas, I. Pérez, T. Rojas, M. E. Valdés-Tresanco, M. Izquierdo, M. A. Del Rivero, Y. M. Álvarez-Ginarte, P. A. Valiente, C. Soto, L. de León, *Eur. J. Med. Chem.* **2019**, *163*, 481.
- [31] T. Budragchaa, B. Westermann, L. A. Wessjohann, *Bioorg. Med. Chem.* **2019**, *27*, 3237.
- [32] H. N. Sultani, H. H. Haeri, D. Hinderberger, B. Westermann, *Org. Biomol. Chem.* **2016**, *14*, 11336.
- [33] H. N. Sultani, I. Morgan, H. Hussain, A. H. Roos, H. H. Haeri, G. N. Kaluderović, D. Hinderberger, B. Westermann, *Int. J. Mol. Sci.* **2021**, *22*, 7125.
- [34] O. Kreye, B. Westermann, L. A. Wessjohann, *Synlett* **2007**, 3188.
- [35] R. A. Neves Filho, S. Stark, M. C. Morejon, B. Westermann, L. A. Wessjohann, *Tetrahedron Lett.* **2012**, *53*, 5360.
- [36] M. Ondar, O. Y. Grinberg, A. Dubinskii, Y. S. Lebedev, *Sov. J. Chem. Phys.* **1985**, *3*, 781.
- [37] W. Snipes, J. Cupp, G. Cohn, A. Keith, *Biophys. J.* **1974**, *14*, 20.
- [38] T. Kawamura, S. Matsunami, T. Yonezawa, *Bull. Chem. Soc. Jpn.* **1967**, *40*, 1111.
- [39] S. Stoll, A. Schweiger, *J. Magn. Reson.* **2006**, *178*, 42.
- [40] T. Taldone, E. M. Gomes-DaGama, H. Zong, S. Sen, M. L. Alpaugh, D. Zatorska, R. Alonso-Sabadell, M. L. Guzman, G. Chiosio, *Bioorg. Med. Chem. Lett.* **2011**, *21*, 5347.